Atmospheric
Chemistry
and Physics
Discussions

Open Access

Impact of gas-to-particle partitioning approaches on the simulated radiative effects of biogenic secondary organic aerosol

C. E. Scott[1], D. V. Spracklen[1], J. R. Pierce[2], I. Riipinen[3], S. D. D'Andrea[2], A. Rap[1], K. S. Carslaw[1], P. M. Forster[1], M. Kulmala[4], G. W. Mann[1,5], and K. J. Pringle[1]

[1]School of Earth and Environment, University of Leeds, Leeds, LS2 9JT, UK
[2]Department of Atmospheric Science, Colorado State University, Ft. Collins, CO, USA
[3]Department of Applied Environmental Science & Bolin Center for Climate Research, Stockholm University, 10691, Stockholm, Sweden
[4]Department of Physics, University of Helsinki, P.O. Box 64, 00014, Finland
[5]National Centre for Atmospheric Science, University of Leeds, Leeds, LS2 9JT, UK

Discussion Paper | Discussion Paper | Discussion Paper | Discussion Paper |

ACPD
15, 4145–4172, 2015

Impact of gas-to-particle partitioning approaches

C. E. Scott et al.

Title Page

Abstract | Introduction
Conclusions | References
Tables | Figures

◄◄ | ►►
◄ | ►

Back | Close

Full Screen / Esc

Printer-friendly Version

Interactive Discussion

C. E. Scott et al.

Abstract

The oxidation of biogenic volatile organic compounds (BVOCs) gives a range of products, from semi-volatile to extremely low-volatility compounds. To treat the interaction of these secondary organic vapours with the particle phase, global aerosol microphysics models generally use either a thermodynamic partitioning approach (assuming instant equilibrium between semi-volatile oxidation products and the particle phase) or a kinetic approach (accounting for the size-dependence of condensation). We show that model treatment of the partitioning of biogenic organic vapours into the particle phase, and consequent distribution of material across the size distribution, controls the magnitude of the first aerosol indirect effect (AIE) due to biogenic secondary organic aerosol (SOA). With a kinetic partitioning approach, SOA is distributed according to the existing condensation sink, enhancing the growth of the smallest particles, i.e., those in the nucleation mode. This process tends to increase cloud droplet number concentrations in the presence of biogenic SOA. By contrast, a thermodynamic approach distributes SOA according to pre-existing organic mass, restricting the growth of the smallest particles, limiting the number that are able to form cloud droplets. With an organically medicated new particle formation mechanism, applying a thermodynamic rather than a kinetic approach reduces our calculated global mean AIE due to biogenic SOA by 24 %. Our results suggest that the mechanisms driving organic partitioning need to be fully understood in order to accurately describe the climatic effects of SOA.

1 Introduction

Biogenic volatile organic compounds (BVOCs), such as monoterpenes and isoprene, are emitted into the atmosphere by vegetation (Guenther et al., 1995, 2006) and are rapidly oxidised. The oxidation of BVOCs yields products with lower volatility, which may partition to the particle phase forming secondary organic aerosol (SOA). Organic compounds contribute a large fraction of submicron aerosol mass (Murphy et al., 2006;

Zhang et al., 2007; Jimenez et al., 2009) with important impacts on air quality and climate (Fiore et al., 2012; Scott et al., 2014).

The part of the aerosol size distribution to which SOA is added affects the number, size and composition of particles in the atmosphere; in particular, the number of particles that are able to act as cloud condensation nuclei (CCN). The availability of CCN controls cloud droplet number concentrations (CDNC), and subsequently cloud albedo; therefore, the manner in which organics are distributed has potential implications for the first aerosol indirect effect (AIE) of biogenic SOA.

The presence of SOA can affect atmospheric CCN concentrations in several ways. Firstly, the condensation of SOA may grow particles to larger sizes, increasing CCN concentrations (Riipinen et al., 2012). However, this enhanced growth increases the condensation sink for potential nucleating vapours, and the coagulation sink for nucleation mode particles. The net change to CCN concentration therefore reflects the competition between particle growth, and the scavenging of particles and vapours. Secondly, condensation of water-soluble organic species can make hydrophobic particles more hydrophilic, providing an additional source of new CCN (Petters et al., 2006).

The transfer of semi-volatile gas-phase organic species into the condensed phase is often treated assuming thermodynamic equilibrium (Pankow, 1994; Odum et al., 1996). When simulating the evolution of the aerosol size distribution, a consequence of assuming instant equilibrium is that the net condensation of new organic mass scales with the existing organic aerosol mass size distribution (Kroll and Seinfeld, 2008; Pierce et al., 2011; Riipinen et al., 2011). Because aerosol mass scales with diameter cubed, small particles that require condensational growth to reach climatically relevant sizes receive only a trivial fraction of the new SOA and subsequently do not grow.

However, if the volatility of organic oxidation products in the atmosphere is further reduced (i.e., through gas or particle-phase chemistry, Jimenez et al., 2009; Donahue et al., 2011; Ehn et al., 2014), they may condense kinetically according to the Fuchs-corrected surface area of existing particles and a larger proportion of the condensable

mass will be added to the nucleation mode (Riipinen et al., 2011; Yu, 2011; Zhang et al., 2012).

Neither approach fully describes the behaviour of SOA; the kinetic approach neglects the re-evaporation of semi-volatile organics whilst the thermodynamic approach is unable to account for the observed growth of particles beyond the nucleation mode (Pierce et al., 2011; Riipinen et al., 2011; Yu, 2011; Pierce et al., 2012). The results of laboratory experiments indicate the presence of both semi-volatile organic aerosol components that evaporate upon heating or dilution (e.g., Robinson et al., 2007) as well as highly oxidised compounds with extremely low volatilities (Ehn et al., 2014) in atmospherically relevant SOA particles.

Global aerosol microphysics models use either the thermodynamic (partitioning proportional to existing organic mass e.g., Chung and Seinfeld, 2002; Heald et al., 2008; Pye and Seinfeld, 2010; O'Donnell et al., 2011) or the kinetic (condensation proportional to particle surface area e.g., Spracklen et al., 2006; Makkonen et al., 2009) assumptions described above. Riipinen et al. (2011) and D'Andrea et al. (2013) both found that the simulated global annual mean concentration of CCN-sized particles increased by approximately 10 % when the kinetic (rather than thermodynamic) assumption was used for SOA, with regional increases of over 50 %. Yu (2011) found that allowing successive stages of oxidation to occur, and the generation of non-volatile products, increased simulated surface level CCN concentrations by 5–50 %, over a version of the same model in which the thermodynamic assumption was applied.

Previous modelling studies have quantified the cloud albedo effect, or first AIE, of biogenic SOA, estimating global annual mean values that span from positive ($+0.23\,\mathrm{W\,m^{-2}}$, O'Donnell et al., 2011) to negative (e.g. $-0.02\,\mathrm{W\,m^{-2}}$, Rap et al., 2013, and $-0.77\,\mathrm{W\,m^{-2}}$, Scott et al., 2014). One difference between these studies is the method by which they represent the condensation of SOA, with O'Donnell et al. (2011) applying a thermodynamic approach whereas the other studies used the kinetic approach. We hypothesise that uncertainty in the sign and magnitude of the first AIE due

Title Page

Abstract	Introduction
Conclusions	References
Tables	Figures

|◀ | ▶|

◀ | ▶

Back | Close

Full Screen / Esc

Printer-friendly Version

Interactive Discussion

to biogenic SOA may, in part, be due to the different approaches used to distribute SOA amongst the existing aerosol population.

Conversely, we hypothesise that the direct radiative effect (DRE) due to biogenic SOA is less sensitive to the way in which secondary organic material is partitioned across the size distribution. Previous studies agree on a negative global annual mean DRE due to biogenic SOA ($-0.29\,\mathrm{W\,m^{-2}}$ (clear-sky; O'Donnell et al., 2011), $-0.13\,\mathrm{W\,m^{-2}}$ (all-sky; Rap et al., 2013), $-0.17\,\mathrm{W\,m^{-2}}$ (all-sky; Unger, 2014) and $-0.18\,\mathrm{W\,m^{-2}}$ (all-sky; Scott et al., 2014)). Rap et al. (2013) explored the radiative effects associated with several natural aerosol sources and demonstrated that the DRE responds linearly to changes in emission source strength and is less sensitive to microphysical complexities than the first AIE.

Here we use a global aerosol microphysics model and offline radiative transfer model to explore how the assumed behaviour of secondary organic material affects simulated changes in CCN-sized particles, and for the first time, CDNC and the radiative effects of biogenic SOA.

2 Method

2.1 GLOMAP

We use the GLObal Model of Aerosol Processes (GLOMAP-mode) (Mann et al., 2010) which is an extension to the TOMCAT model (Chipperfield, 2006). GLOMAP operates at a horizontal resolution of $2.8° \times 2.8°$ with 31σ-pressure levels from the surface to 10 hPa. Meteorology is obtained from European Centre for Medium-Range Weather Forecasts (ECMWF) reanalyses at six-hourly intervals and cloud fields from the International Satellite Cloud Climatology Project (ISCCP) archive (Rossow and Schiffer, 1999). The particle component masses and number concentrations are simulated in 5 log-normal size modes; four hydrophilic (nucleation, Aitken, accumulation and coarse), and a non-hydrophilic Aitken mode. Material in the particle-phase is classi-

fied into four components: sulphate (SU), black carbon (BC), particulate organic matter (POM) and sea-salt (SS). GLOMAP includes representations of nucleation, particle growth via coagulation, condensation and cloud processing, wet and dry deposition and in/below cloud scavenging. We prescribe six-hourly mean offline oxidant (OH, O_3, NO_3, HO_2, H_2O_2) concentrations from a previous TOMCAT simulation (Arnold et al., 2005). Monoterpene emissions are taken from the Global Emissions InitiAtive (GEIA) database (Guenther et al., 1995) and secondary organic material is generated at a fixed molar yield (13 %) from the oxidation of monoterpenes by O_3, OH and NO_3; producing approximately $20\,\mathrm{Tg\,(SOA)\,a^{-1}}$. Further details of this model setup are given in Scott et al. (2014).

2.1.1 New particle formation

All model experiments include a representation of binary homogeneous nucleation (BHN), which simulates the formation of particles from H_2SO_4 and H_2O; this occurs predominantly in the free troposphere, and is parameterised according to Kulmala et al. (1998). One set of experiments (ACT; Table 1), use an empirically derived mechanism for the activation rate (J^*_{ACT}) of H_2SO_4 clusters in the boundary layer (Eq. 1; Kulmala et al., 2006), with a value for A of $2 \times 10^{-6}\,\mathrm{s^{-1}}$ (Sihto et al., 2006).

$$J^*_{ACT} = A[H_2SO_4] \tag{1}$$

In a second set of experiments (ORG; Table 1), new particle formation is parameterised according to Metzger et al. (2010). In these simulations, the cluster formation rate (J^*_{ORG}) is calculated according to Eq. (2), where NucOrg represents monoterpene oxidation products and $k = 5 \times 10^{-13}\,\mathrm{s^{-1}}$ (Metzger et al., 2010).

$$J^*_{ORG} = k[H_2SO_4][NucOrg] \tag{2}$$

The initial stages of cluster growth are not simulated explicitly, rather the approximation of Kerminen and Kulmala (2002) as given in Eq. (3), is used to determine the

production rate (J_m) of particles at a measurable size (taken as $d_m = 3\,\mathrm{nm}$). The cluster dry-diameter (d^*) is taken as 0.8 nm for J^*_{ACT} and 1.5 nm for J^*_{ORG} (Metzger et al., 2010).

$$J_m = J^* \exp\left[0.23 \left(\frac{1}{d_m} - \frac{1}{d^*} \right) \frac{CS'}{GR} \right] \tag{3}$$

J_m allows the growth of newly formed clusters (up to d_m) at a constant growth rate (GR); here GR is proportional to the gas-phase concentration of sulphuric acid, but other species could also contribute to growth at this size (Yli-Juuti et al., 2011; Kulmala et al., 2013). J_m also accounts for the scavenging of newly formed clusters by larger particles; the reduced condensation sink (CS$'$) is calculated by integrating over the aerosol size modes, following Kulmala et al. (2001).

2.1.2 Partitioning of secondary organic material

The rate of change of gas-phase molecular concentration of organics (S_{org}) due to condensation is calculated as in Eq. (4) where C_i is the condensation coefficient for each mode i (Eq. 5) and N_i is the corresponding particle number concentration. C_i is calculated for each mode i as described in Mann et al. (2010) using the diffusion coefficient for a typical gas-phase α-pinene oxidation product in air (D_s) and the condensation sink radius ($\overline{r_{i,\,cond}}$, calculated as in Eq. (A1) of Mann et al. (2012) which is based on Lehtinen et al., 2003). C_i is corrected for molecular effects and limitations in interfacial mass transport by the terms $F(Kn_i)$ and $A(Kn_i)$ respectively (Eqs. 6 and 7), where s is the accommodation coefficient, or sticking efficiency. Here we assume a value of s equal to 1, therefore $A(Kn_i)$ is unity in this case. Kn_i is the Knudsen number for each mode i (Eq. 8), calculated using the mean free path of the relevant condensable gas in

air (MFP$_{gas}$).

$$\frac{dS_{org}}{dt} = -\left(\sum_i C_i N_i\right) S_{org} \tag{4}$$

$$C_i = 4\pi D_s \overline{r_{i,cond}} F(Kn_i) A(Kn_i) \tag{5}$$

$$F(Kn_i) = \frac{1 + Kn_i}{1 + 1.71Kn_i + 1.33(Kn_i)^2} \tag{6}$$

$$A(Kn_i) = \frac{1}{1 + 1.33Kn_i F(Kn_i)\left(\frac{1}{s} - 1\right)} \tag{7}$$

$$Kn_i = \frac{MFP_{gas}}{r_{i,cond}} \tag{8}$$

We apply two different approaches to distribute SOA across the pre-existing aerosol size distribution. In GLOMAP the standard approach is to assume secondary organic mass (M_{SOA}) condenses as if it were non-volatile, to the Fuchs-corrected surface area (i.e., the kinetic approach) as in Eq. (9).

$$\frac{dM_{SOA_i}}{dt} = \frac{C_i N_i}{\sum_{i=1,5} C_i N} \times \frac{dS_{org}}{dt} \tag{9}$$

Here, we apply a second approach in which the amount of secondary organic material entering the aerosol phase is partitioned between the size modes according to Eq. (10), mimicking the thermodynamic approach; M_{OAi} is the pre-existing organic mass in mode i.

$$\frac{dM_{SOA_i}}{dt} = \frac{M_{OA_i}}{\sum_{i=1,5} M_{OA_i}} \times \frac{dS_{org}}{dt} \tag{10}$$

4152

Title Page

Abstract | Introduction

Conclusions | References

Tables | Figures

◀ | ▶

◀ | ▶

Back | Close

Full Screen / Esc

Printer-friendly Version

Interactive Discussion

Because our aim is to quantify the impact of changes in the size of particles to which the SOA condenses we otherwise treat SOA identically between the two different approaches and do not allow SOA to re-partition into the gas phase.

We complete one simulation without biogenic SOA (NoSOA), as well as simulations with biogenic SOA distributed according to the kinetic approach (KinSOA), the thermodynamic approach (ThermSOA), and a simulation in which 50 % of the SOA mass is distributed according to each approach (SplitSOA).

2.2 Calculation of radiative effects

The changes to CDNC due to the inclusion of biogenic SOA (i.e., KinSOA – NoSOA) are calculated using the parameterisation developed by Nenes and Seinfeld (2003), and updated by Fountoukis and Nenes (2005) and Barahona et al. (2010), with a globally uniform updraught velocity of $0.2\,\mathrm{m\,s^{-1}}$.

The first AIE of biogenic SOA is then determined using the offline radiative transfer model of Edwards and Slingo (1996) with nine bands in the longwave and six bands in the shortwave; a monthly mean climatology based on ECMWF reanalysis data and cloud fields for the year 2000 from the ISCCP-D2 archive (Rossow and Schiffer, 1999) are used. To calculate the first AIE, a uniform control cloud droplet effective radius (r_{e1}) of $10\,\mu\mathrm{m}$ is assumed, to maintain consistency with the ISCCP derivation of liquid water path, and for each perturbation experiment the effective radius (r_{e2}) is calculated as in Eq. (11), from cloud droplet number fields $CDNC_1$ and $CDNC_2$ respectively (where $CDNC_1$ represents the simulation including SOA, and $CDNC_2$ represents the simulation with no SOA). Only the effective radii of low- and mid-level (below $600\,\mathrm{hPa}$) water clouds are modified.

$$r_{e2} = r_{e1} \times \left[\frac{CDNC_1}{CDNC_2} \right]^{\frac{1}{3}} \qquad (11)$$

The first AIE of biogenic SOA is then calculated by comparing net (SW + LW) radiative fluxes using the varying r_{e2} values derived for each perturbation experiment, to those

of the control simulation with fixed r_{e1}. In these offline experiments, we do not calculate the second aerosol indirect (cloud lifetime) effect.

To determine the DRE, following the methodology described in Rap et al. (2013), the radiative transfer model is used to calculate the difference in net top-of-atmosphere all-sky radiative flux between experiments including SOA and the equivalent experiments without SOA. Aerosol scattering and absorption coefficients together with asymmetry parameters are calculated for each aerosol size mode and spectral band, based on the volume-weighted mean refractive index (taken from Table A1 of Bellouin et al., 2011) of the components present, as described in Bellouin et al. (2013).

3   Results

Table 1 summarises how the treatment of SOA condensation in GLOMAP impacts the global flux of secondary organic material to the aerosol size distribution. The total global flux of secondary organic material to the particle phase is the same in each approach ($\sim 20.2\,\mathrm{Tg\,(SOA)\,a^{-1}}$), but there are important changes to how the material is distributed across particles of different sizes. When the thermodynamic approach is applied, no SOA is added to the nucleation mode. Rather, SOA is added to larger particles with greater existing organic mass (more than 80 % to particles with dry diameter greater than 100 nm, less than 20 % to particles with dry diameter between 10 and 100 nm). Under the kinetic approach, most of the secondary organic material also condenses on the larger particles (~ 74–78 % to particles with diameter greater than 100 nm, ~ 21–24 % to particles with dry diameter between 10 and 100 nm). Additionally, a small fraction (0.26–0.87 %) of secondary organic material is added to the nucleation mode (i.e., particles with diameter less than 10 nm), under the kinetic approach. As we show below, this small amount of SOA (0.05–$0.18\,\mathrm{Tg\,(SOA)\,a^{-1}}$) adding to nucleation mode particles has important implications for the aerosol size distribution.

Figure 1 compares simulated and observed aerosol size distributions at a boreal forest location (Hyytiälä, Finland (24.3° E, 61.9° N; described in Hari and Kulmala, 2005)).

At Hyytiälä, the simulated aerosol size distribution is sensitive to a range of processes including particle formation rates, amount of SOA and the characteristics of primary particles (e.g., Spracklen et al., 2008, 2010; Reddington et al., 2011). Our intention here is to demonstrate that the aerosol size distribution is also sensitive to the treatment of SOA condensation.

When the thermodynamic approach (ThermSOA; dashed lines in Fig. 1) is applied, the model simulates high concentrations of nucleation mode particles (smaller than 10 nm dry diameter). Under this approach no organic material condenses on these small particles and their growth is slow since it is limited by the availability of sulphuric acid (Riipinen et al., 2011). This slow growth rate means few particles can grow to larger sizes and the number of particles between 30–100 nm diameter is far less than observed. When the kinetic approach is applied, a small amount of SOA condenses onto particles in the nucleation mode (0.26 % of the total flux for ACT and 0.87 % for ORG; Table 1), increasing the growth rate of these small particles. The kinetic approach results in a greater number of particles in the 30–100 nm size range compared to the thermodynamic approach, improving the match against observations over this size range (KinSOA; full lines in Fig. 1).

We find the best match between model and observations when we assume organically mediated new particle formation and kinetic condensation of organic material (KinSOA_ORG; full red lines in Fig. 1). The faster nucleation rates under this mechanism combined with condensation of organic material on small particles under the kinetic condensation assumption increases the number of particles in the 30–100 nm size range. The same relative response to the kinetic and thermodynamic approaches was documented by D'Andrea et al. (2013) and is consistent with the findings of Yu (2011).

In the SplitSOA experiments, some secondary organic material is able to condense onto newly formed particles (0.19 % of the total flux for ACT and 0.67 % for ORG; Table 1), resulting in a size distribution similar to that generated by the kinetic approach (SplitSOA; dotted lines in Fig. 1). This implies that it is not necessary to assume that

all of the organic material generated has an extremely low volatility in order to account for the observed growth, but that some fraction of the SOA does need to be treated in this way, consistent with the findings of Kulmala et al. (2013).

3.1 Changes to cloud droplet number concentration

Table 2 reports the simulated changes to global CDNC due to biogenic SOA under the kinetic, thermodynamic and split approaches, for both nucleation mechanisms. As we have reported previously, the impact of biogenic SOA on CDNC strongly depends on the nucleation mechanism used in the model, with the largest impact on CDNC simulated with an organically mediated new particle formation mechanism (Scott et al., 2014). We find that for both nucleation mechanisms, biogenic SOA leads to a larger global annual mean increase in CDNC under the kinetic condensation approach compared to the thermodynamic approach. With the ACT nucleation mechanism, GLOMAP simulates a 3.4 % increase in global annual mean CDNC with kinetic condensation but only a 1.4 % increase with thermodynamic condensation. Similarly, with the ORG nucleation mechanism, GLOMAP simulates a 25.1 % increase in global annual mean CDNC with kinetic condensation and a 20.0 % increase with thermodynamic condensation. The SplitSOA approach increases the global annual mean CDNC by almost as much as the kinetic approach (+3.2 % for ACT and +24.4 % for ORG) because only a small amount of SOA is required to allow the smallest particles to grow sufficiently.

Simulated changes to CDNC are not restricted to the areas over which biogenic SOA is generated, or proportional to the amount of SOA being generated (Fig. 2), as discussed in Scott et al. (2014). Under the kinetic approach, GLOMAP simulates large fractional increases to CDNC over boreal regions and Southern Hemisphere oceans (greater than 20 % for ACT and over 100 % for ORG; Fig. 2). Under the thermodynamic approach, the growth of particles to CCN-relevant size is suppressed and fewer regions experience such large increases in CDNC in response to the inclusion of biogenic SOA.

The inclusion of biogenic SOA can induce decreases in simulated CDNC due to an enhanced rate of ageing/scavenging of initially hydrophobic particles, or the suppres-

sion of nucleation in the free troposphere (and subsequent entrainment back into the boundary layer) due to an increased condensation sink at the surface (Scott et al., 2014). When the ACT mechanism for new particle formation is used with the kinetic approach, these effects combine to give small decreases to CDNC over tropical ocean
⁵ regions (Fig. 2a); when the thermodynamic approach is used, much larger ocean regions experience a decrease in CDNC (Fig. 2b). In the ORG simulations, the contribution of organic oxidation products to new particle formation is sufficient to prevent any regional decreases in CDNC under either approach (Fig. 2c and d).

To examine the sensitivity of this response to updraught velocity, CDNC were cal-
¹⁰ culated at five globally uniform updraught velocities, from 0.1 to 0.5 m s^{-1}, for the ACT set of experiments (Table 3). Under both approaches to SOA partitioning, increasing the updraught velocity increases the absolute and fractional change in CDNC at low-level cloud base due to biogenic SOA; however, the relative kinetic to thermodynamic response remains consistent.

¹⁵ ## 3.2 First aerosol indirect effect

We explored the impact of the condensation approach on the first AIE due to biogenic SOA and report the global annual mean values in Table 2; Fig. 3 shows the spatial patterns in annual mean first AIE for each nucleation mechanism and partitioning assumption. The global annual mean first AIE is calculated for an updraft velocity of 0.2 m s^{-1};
²⁰ in Table 3 we show consistent results for a range of updraft velocities between 0.1 and 0.5 m s^{-1}.

Increases in CDNC lead to a negative first AIE (i.e., a cooling effect), and decreases in CDNC lead to a positive first AIE (i.e., a warming effect). When the ACT new particle formation mechanism is used, the kinetic approach gives a negative global annual
²⁵ mean first AIE of −0.07 W m^{-2}, with a negative first AIE in regions of CDNC increase, and a positive first AIE in regions of CDNC decrease (Fig. 3a). When the ACT mechanism is used with the thermodynamic approach, spatially extensive decreases in CDNC (as compared to the kinetic approach) lead to large regions where a positive first AIE is

simulated, and a positive global annual mean first AIE ($+0.01\,\mathrm{W\,m^{-2}}$) due to biogenic SOA (Fig. 3b).

When the ORG mechanism is used with the kinetic approach, the inclusion of biogenic SOA generates a global annual mean first AIE of $-0.78\,\mathrm{W\,m^{-2}}$, due to widespread increases in CDNC (Fig. 2c), which is reduced to $-0.59\,\mathrm{W\,m^{-2}}$ under the thermodynamic approach (Table 2). A global annual mean negative first AIE is maintained under the thermodynamic approach because the contribution of organic oxidation products to new particle formation is sufficient to outweigh the impact of suppressed growth on CDNC (Fig. 2d).

For both nucleation mechanisms, the SplitSOA approach gives a negative first AIE ($-0.05\,\mathrm{W\,m^{-2}}$ for ACT and $-0.75\,\mathrm{W\,m^{-2}}$ for ORG), of similar magnitude to the kinetic approach due to similar changes to global annual mean CDNC.

3.3 Direct radiative effect

The direct radiative effect is less sensitive to the distribution of secondary organic material across the aerosol size distribution (Table 2). When the ACT new particle formation mechanism is used, the kinetic approach gives a global annual mean DRE of $-0.10\,\mathrm{W\,m^{-2}}$, as compared to $-0.11\,\mathrm{W\,m^{-2}}$ with the kinetic approach. When the ORG mechanism for new particle formation is used, the inclusion of biogenic SOA generates a global annual mean DRE of $-0.08\,\mathrm{W\,m^{-2}}$ under both the kinetic and thermodynamic approaches.

This lack of sensitivity can be explained in part by the fact that, under the thermodynamic approach, the shift in SOA mass from smaller ($< 100\,\mathrm{nm}$ dry diameter) to larger ($> 100\,\mathrm{nm}$ dry diameter) particles represents a much smaller fractional change to the amount of SOA the larger particles receive. Using the ACT mechanism, particles greater than 100 nm dry diameter receive 20 % more secondary organic mass per particle under the thermodynamic approach, relative to the amount they received under the kinetic approach. Whereas, particles smaller than 100 nm dry diameter receive

40 % less secondary organic mass per particle under the thermodynamic approach, relative to the amount they received under the kinetic approach (Table 2).

4   Conclusions

Using a global aerosol microphysics model we have shown that the manner in which secondary organic material is added to the aerosol size distribution is important in determining its impact on the number and size of climatically relevant particles in the atmosphere.

The kinetic approach to partitioning, which enables organic oxidation products to condense upon the smallest particles, facilitating their growth to larger sizes, increases global annual mean CDNC when either an activation or organically mediated new particle formation mechanism is applied (by 3.4 % for ACT and 25.1 % for ORG). These global annual mean increases in CDNC result in a negative global annual mean first AIE ($-0.07\,\mathrm{W\,m^{-2}}$ for ACT and $-0.78\,\mathrm{W\,m^{-2}}$ for ORG).

Applying the thermodynamic approach suppresses the growth of the smallest particles, resulting in a smaller global annual mean increase in CDNC (+1.4 % for ACT and +20.0 % for ORG). When an activation mechanism is applied to new particle formation, the thermodynamic approach results in a small positive first AIE ($+0.01\,\mathrm{W\,m^{-2}}$) due to biogenic SOA. When an organically mediated new particle formation mechanism is applied, a negative first AIE is maintained because the contribution of organic oxidation products to new particle formation is sufficient to outweigh the impact of suppressed growth on CDNC, but the magnitude of the first AIE is reduced to $-0.59\,\mathrm{W\,m^{-2}}$.

Neither approach adequately describes the complex behaviour of secondary organic material in the atmosphere. Ultimately, a combination of the thermodynamic and kinetic approaches will be required to accurately represent the behaviour of SOA in global models. Improving on existing first attempts by e.g., Riipinen et al. (2011), Yu (2011), and the SplitSOA approach described here, will require a more detailed understanding

Title Page

Abstract | Introduction

Conclusions | References

Tables | Figures

◀ | ▶

◀ | ▶

Back | Close

Full Screen / Esc

Printer-friendly Version

Interactive Discussion

of the pathways by which organic compounds of differing volatilities are generated, and their relative contributions to the growth of particles of different sizes.

References

Arnold, S. R., Chipperfield, M. P., and Blitz, M. A.: A three-dimensional model study of the effect of new temperature-dependent quantum yields for acetone photolysis, J. Geophys. Res., 110, D22305, doi:10.1029/2005jd005998, 2005.

Barahona, D., West, R. E. L., Stier, P., Romakkaniemi, S., Kokkola, H., and Nenes, A.: Comprehensively accounting for the effect of giant CCN in cloud activation parameterizations, Atmos. Chem. Phys., 10, 2467–2473, doi:10.5194/acp-10-2467-2010, 2010.

Bellouin, N., Rae, J., Jones, A., Johnson, C., Haywood, J., and Boucher, O.: Aerosol forcing in the Climate Model Intercomparison Project (CMIP5) simulations by HadGEM2-ES and the role of ammonium nitrate, J. Geophys. Res., 116, D20206, doi:10.1029/2011jd016074, 2011.

Bellouin, N., Mann, G. W., Woodhouse, M. T., Johnson, C., Carslaw, K. S., and Dalvi, M.: Impact of the modal aerosol scheme GLOMAP-mode on aerosol forcing in the Hadley Centre Global Environmental Model, Atmos. Chem. Phys., 13, 3027–3044, doi:10.5194/acp-13-3027-2013, 2013.

Chipperfield, M. P.: New version of the TOMCAT/SLIMCAT off-line chemical transport model: intercomparison of stratospheric tracer experiments, Q. J. Roy. Meteor. Soc., 132, 1179–1203, doi:10.1256/qj.05.51, 2006.

Chung, S. H. and Seinfeld, J. H.: Global distribution and climate forcing of carbonaceous aerosols, J. Geophys. Res., 107, 4407, doi:10.1029/2001jd001397, 2002.

D'Andrea, S. D., Häkkinen, S. A. K., Westervelt, D. M., Kuang, C., Levin, E. J. T., Kanawade, V. P., Leaitch, W. R., Spracklen, D. V., Riipinen, I., and Pierce, J. R.: Understanding global secondary organic aerosol amount and size-resolved condensational behavior, Atmos. Chem. Phys., 13, 11519–11534, doi:10.5194/acp-13-11519-2013, 2013.

Donahue, N. M., Trump, E. R., Pierce, J. R., and Riipinen, I.: Theoretical constraints on pure vapor-pressure driven condensation of organics to ultrafine particles, Geophys. Res. Lett., 38, L16801, doi:10.1029/2011gl048115, 2011.

Edwards, J. M. and Slingo, A.: Studies with a flexible new radiation code. I: Choosing a configuration for a large-scale model, Q. J. Roy. Meteor. Soc., 122, 689–719, doi:10.1002/qj.49712253107, 1996.

Ehn, M., Thornton, J. A., Kleist, E., Sipila, M., Junninen, H., Pullinen, I., Springer, M., Rubach, F., Tillmann, R., Lee, B., Lopez-Hilfiker, F., Andres, S., Acir, I.-H., Rissanen, M., Jokinen, T., Schobesberger, S., Kangasluoma, J., Kontkanen, J., Nieminen, T., Kurten, T., Nielsen, L. B., Jorgensen, S., Kjaergaard, H. G., Canagaratna, M., Maso, M. D., Berndt, T., Petaja, T., Wahner, A., Kerminen, V.-M., Kulmala, M., Worsnop, D. R., Wildt, J., and Mentel, T. F.: A large source of low-volatility secondary organic aerosol, Nature, 506, 476–479, doi:10.1038/nature13032, 2014.

Fiore, A. M., Naik, V., Spracklen, D. V., Steiner, A., Unger, N., Prather, M., Bergmann, D., Cameron-Smith, P. J., Cionni, I., Collins, W. J., Dalsoren, S., Eyring, V., Folberth, G. A., Ginoux, P., Horowitz, L. W., Josse, B., Lamarque, J.-F., MacKenzie, I. A., Nagashima, T., O'Connor, F. M., Righi, M., Rumbold, S. T., Shindell, D. T., Skeie, R. B., Sudo, K., Szopa, S., Takemura, T., and Zeng, G.: Global air quality and climate, Chem. Soc. Rev., 41, 6663–6683, doi:10.1039/c2cs35095e, 2012.

Fountoukis, C. and Nenes, A.: Continued development of a cloud droplet formation parameterization for global climate models, J. Geophys. Res., 110, D11212, doi:10.1029/2004jd005591, 2005.

Guenther, A., Hewitt, C. N., Erickson, D., Fall, R., Geron, C., Graedel, T., Harley, P., Klinger, L., Lerdau, M., McKay, W. A., Pierce, T., Scholes, B., Steinbrecher, R., Tallamraju, R., Taylor, J., and Zimmerman, P.: A global model of natural volatile organic compound emissions, J. Geophys. Res., 100, 8873–8892, doi:10.1029/94jd02950, 1995.

Guenther, A., Karl, T., Harley, P., Wiedinmyer, C., Palmer, P. I., and Geron, C.: Estimates of global terrestrial isoprene emissions using MEGAN (Model of Emissions of Gases and Aerosols from Nature), Atmos. Chem. Phys., 6, 3181–3210, doi:10.5194/acp-6-3181-2006, 2006.

Hari, P. and Kulmala, M.: Station for measuring ecosystem-atmosphere relations (SMEAR II), Boreal Environ. Res., 10, 315–322, 2005.

Heald, C. L., Henze, D. K., Horowitz, L. W., Feddema, J., Lamarque, J. F., Guenther, A., Hess, P. G., Vitt, F., Seinfeld, J. H., Goldstein, A. H., and Fung, I.: Predicted change in global secondary organic aerosol concentrations in response to future climate, emissions, and land use change, J. Geophys. Res., 113, D05211, doi:10.1029/2007jd009092, 2008.

Jimenez, J. L., Canagaratna, M. R., Donahue, N. M., Prevot, A. S. H., Zhang, Q., Kroll, J. H., DeCarlo, P. F., Allan, J. D., Coe, H., Ng, N. L., Aiken, A. C., Docherty, K. S., Ulbrich, I. M., Grieshop, A. P., Robinson, A. L., Duplissy, J., Smith, J. D., Wilson, K. R., Lanz, V. A., Hueglin, C., Sun, Y. L., Tian, J., Laaksonen, A., Raatikainen, T., Rautiainen, J., Vaattovaara, P., Ehn, M., Kulmala, M., Tomlinson, J. M., Collins, D. R., Cubison, M. J., E., Dunlea, J., Huffman, J. A., Onasch, T. B., Alfarra, M. R., Williams, P. I., Bower, K., Kondo, Y., Schneider, J., Drewnick, F., Borrmann, S., Weimer, S., Demerjian, K., Salcedo, D., Cottrell, L., Griffin, R., Takami, A., Miyoshi, T., Hatakeyama, S., Shimono, A., Sun, J. Y., Zhang, Y. M., Dzepina, K., Kimmel, J. R., Sueper, D., Jayne, J. T., Herndon, S. C., Trimborn, A. M., Williams, L. R., Wood, E. C., Middlebrook, A. M., Kolb, C. E., Baltensperger, U., and Worsnop, D. R.: Evolution of organic aerosols in the atmosphere, Science, 326, 1525–1529, doi:10.1126/science.1180353, 2009.

Kerminen, V.-M., and Kulmala, M.: Analytical formulae connecting the "real" and the "apparent" nucleation rate and the nuclei number concentration for atmospheric nucleation events, J. Aerosol Sci., 33, 609–622, doi:10.1016/s0021-8502(01)00194-x, 2002.

Kroll, J. H. and Seinfeld, J. H.: Chemistry of secondary organic aerosol: formation and evolution of low-volatility organics in the atmosphere, Atmos. Environ., 42, 3593–3624, 2008.

Kulmala, M., Laaksonen, A., and Pirjola, L.: Parameterisations for sulphuric acid/water nucleation rates, J. Geophys. Res.-Atmos., 103, 8301–8307, doi:10.1029/97JD03718, 1998.

Kulmala, M., Maso, M. D., Mäkelä, J. M., Pirjola, L., Väkevä, M., Aalto, P., Miikkulainen, P., Hämeri, K., and O'Dowd, C. D.: On the formation, growth and composition of nucleation mode particles, Tellus B, 53, 479–490, doi:10.1034/j.1600-0889.2001.530411.x, 2001.

Kulmala, M., Lehtinen, K. E. J., and Laaksonen, A.: Cluster activation theory as an explanation of the linear dependence between formation rate of 3nm particles and sulphuric acid concentration, Atmos. Chem. Phys., 6, 787–793, doi:10.5194/acp-6-787-2006, 2006.

Kulmala, M., Kontkanen, J., Junninen, H., Lehtipalo, K., Manninen, H. E., Nieminen, T., Petäjä, T., Sipilä, M., Schobesberger, S., Rantala, P., Franchin, A., Jokinen, T., Järvinen, E., Äijälä, M., Kangasluoma, J., Hakala, J., Aalto, P. P., Paasonen, P., Mikkilä, J., Vanhanen, J., Aalto, J., Hakola, H., Makkonen, U., Ruuskanen, T., Mauldin, R. L., Du-

plissy, J., Vehkamäki, H., Bäck, J., Kortelainen, A., Riipinen, I., Kurtén, T., Johnston, M. V., Smith, J. N., Ehn, M., Mentel, T. F., Lehtinen, K. E. J., Laaksonen, A., Kerminen, V.-M., and Worsnop, D. R.: Direct observations of atmospheric aerosol nucleation, Science, 339, 943–946, doi:10.1126/science.1227385, 2013.

5   Lehtinen, K. E. J., Korhonen, H., Dal Maso, M., and Kulmala, M.: On the concept of condensation sink diameter, Boreal Environ. Res., 8, 405–411, 2003.

Makkonen, R., Asmi, A., Korhonen, H., Kokkola, H., Järvenoja, S., Räisänen, P., Lehtinen, K. E. J., Laaksonen, A., Kerminen, V.-M., Järvinen, H., Lohmann, U., Bennartz, R., Feichter, J., and Kulmala, M.: Sensitivity of aerosol concentrations and cloud properties to 10   nucleation and secondary organic distribution in ECHAM5-HAM global circulation model, Atmos. Chem. Phys., 9, 1747–1766, doi:10.5194/acp-9-1747-2009, 2009.

Mann, G. W., Carslaw, K. S., Spracklen, D. V., Ridley, D. A., Manktelow, P. T., Chipperfield, M. P., Pickering, S. J., and Johnson, C. E.: Description and evaluation of GLOMAP-mode: a modal global aerosol microphysics model for the UKCA composition-climate model, Geosci. Model 15   Dev., 3, 519–551, doi:10.5194/gmd-3-519-2010, 2010.

Mann, G. W., Carslaw, K. S., Ridley, D. A., Spracklen, D. V., Pringle, K. J., Merikanto, J., Korhonen, H., Schwarz, J. P., Lee, L. A., Manktelow, P. T., Woodhouse, M. T., Schmidt, A., Breider, T. J., Emmerson, K. M., Reddington, C. L., Chipperfield, M. P., and Pickering, S. J.: Intercomparison of modal and sectional aerosol microphysics representations within the same 20   3-D global chemical transport model, Atmos. Chem. Phys., 12, 4449–4476, doi:10.5194/acp-12-4449-2012, 2012.

Metzger, A., Verheggen, B., Dommen, J., Duplissy, J., Prevot, A. S. H., Weingartner, E., Riipinen, I., Kulmala, M., Spracklen, D. V., Carslaw, K. S., and Baltensperger, U.: Evidence for the role of organics in aerosol particle formation under atmospheric conditions, P. Natl. Acad. 25   Sci. USA, 107, 6646–6651, doi:10.1073/pnas.0911330107, 2010.

Murphy, D. M., Cziczo, D. J., Froyd, K. D., Hudson, P. K., Matthew, B. M., Middlebrook, A. M., Peltier, R. E., Sullivan, A., Thomson, D. S., and Weber, R. J.: Single-particle mass spectrometry of tropospheric aerosol particles, J. Geophys. Res.-Atmos., 111, D23S32, doi:10.1029/2006jd007340, 2006.

30   Nenes, A. and Seinfeld, J. H.: Parameterization of cloud droplet formation in global climate models, J. Geophys. Res., 108, 4415, doi:10.1029/2002JD002911, 2003.

O'Donnell, D., Tsigaridis, K., and Feichter, J.: Estimating the direct and indirect effects of secondary organic aerosols using ECHAM5-HAM, Atmos. Chem. Phys., 11, 8635–8659, doi:10.5194/acp-11-8635-2011, 2011.

Odum, J. R., Hoffmann, T., Bowman, F., Collins, D., Flagan, R. C., and Seinfeld, J. H.: Gas/particle partitioning and secondary organic aerosol yields, Environ. Sci. Technol., 30, 2580–2585, doi:10.1021/es950943+, 1996.

Pankow, J. F.: An absorption model of the gas/aerosol partitioning involved in the formation of secondary organic aerosol, Atmos. Environ., 28, 189–193, doi:10.1016/1352-2310(94)90094-9, 1994.

Petters, M. D., Prenni, A. J., Kreidenweis, S. M., DeMott, P. J., Matsunaga, A., Lim, Y. B., and Ziemann, P. J.: Chemical aging and the hydrophobic-to-hydrophilic conversion of carbonaceous aerosol, Geophys. Res. Lett., 33, L24806, doi:10.1029/2006gl027249, 2006.

Pierce, J. R., Riipinen, I., Kulmala, M., Ehn, M., Petäjä, T., Junninen, H., Worsnop, D. R., and Donahue, N. M.: Quantification of the volatility of secondary organic compounds in ultrafine particles during nucleation events, Atmos. Chem. Phys., 11, 9019–9036, doi:10.5194/acp-11-9019-2011, 2011.

Pierce, J. R., Leaitch, W. R., Liggio, J., Westervelt, D. M., Wainwright, C. D., Abbatt, J. P. D., Ahlm, L., Al-Basheer, W., Cziczo, D. J., Hayden, K. L., Lee, A. K. Y., Li, S.-M., Russell, L. M., Sjostedt, S. J., Strawbridge, K. B., Travis, M., Vlasenko, A., Wentzell, J. J. B., Wiebe, H. A., Wong, J. P. S., and Macdonald, A. M.: Nucleation and condensational growth to CCN sizes during a sustained pristine biogenic SOA event in a forested mountain valley, Atmos. Chem. Phys., 12, 3147–3163, doi:10.5194/acp-12-3147-2012, 2012.

Pye, H. O. T. and Seinfeld, J. H.: A global perspective on aerosol from low-volatility organic compounds, Atmos. Chem. Phys., 10, 4377–4401, doi:10.5194/acp-10-4377-2010, 2010.

Rap, A., Scott, C. E., Spracklen, D. V., Bellouin, N., Forster, P. M., Carslaw, K. S., Schmidt, A., and Mann, G.: Natural aerosol direct and indirect radiative effects, Geophys. Res. Lett., 40, 3297–3301, doi:10.1002/grl.50441, 2013.

Reddington, C. L., Carslaw, K. S., Spracklen, D. V., Frontoso, M. G., Collins, L., Merikanto, J., Minikin, A., Hamburger, T., Coe, H., Kulmala, M., Aalto, P., Flentje, H., Plass-Dülmer, C., Birmili, W., Wiedensohler, A., Wehner, B., Tuch, T., Sonntag, A., O'Dowd, C. D., Jennings, S. G., Dupuy, R., Baltensperger, U., Weingartner, E., Hansson, H.-C., Tunved, P., Laj, P., Sellegri, K., Boulon, J., Putaud, J.-P., Gruening, C., Swietlicki, E., Roldin, P., Henzing, J. S., Moerman, M., Mihalopoulos, N., Kouvarakis, G., Ždímal, V., Zíková, N., Marinoni, A., Bonasoni, P.,

Title Page

Abstract · Introduction

Conclusions · References

Tables · Figures

◄ · ►

◄ · ►

Back · Close

Full Screen / Esc

Printer-friendly Version

Interactive Discussion

and Duchi, R.: Primary versus secondary contributions to particle number concentrations in the European boundary layer, Atmos. Chem. Phys., 11, 12007–12036, doi:10.5194/acp-11-12007-2011, 2011.

Riipinen, I., Pierce, J. R., Yli-Juuti, T., Nieminen, T., Häkkinen, S., Ehn, M., Junninen, H., Lehtipalo, K., Petäjä, T., Slowik, J., Chang, R., Shantz, N. C., Abbatt, J., Leaitch, W. R., Kerminen, V.-M., Worsnop, D. R., Pandis, S. N., Donahue, N. M., and Kulmala, M.: Organic condensation: a vital link connecting aerosol formation to cloud condensation nuclei (CCN) concentrations, Atmos. Chem. Phys., 11, 3865–3878, doi:10.5194/acp-11-3865-2011, 2011.

Riipinen, I., Yli-Juuti, T., Pierce, J. R., Petäjä, T., Worsnop, D. R., Kulmala, M., and Donahue, N. M.: The contribution of organics to atmospheric nanoparticle growth, Nat. Geosci., 5, 453–458, doi:10.1038/ngeo1499, 2012.

Robinson, A. L., Donahue, N. M., Shrivastava, M. K., Weitkamp, E. A., Sage, A. M., Grieshop, A. P., Lane, T. E., Pierce, J. R., and Pandis, S. N.: Rethinking organic aerosols: semivolatile emissions and photochemical aging, Science, 315, 1259–1262, doi:10.1126/science.1133061, 2007.

Rossow, W. B. and Schiffer, R. A.: Advances in understanding clouds from ISCCP, B. Am. Meteorol. Soc., 80, 2261–2287, 1999.

Scott, C. E., Rap, A., Spracklen, D. V., Forster, P. M., Carslaw, K. S., Mann, G. W., Pringle, K. J., Kivekäs, N., Kulmala, M., Lihavainen, H., and Tunved, P.: The direct and indirect radiative effects of biogenic secondary organic aerosol, Atmos. Chem. Phys., 14, 447–470, doi:10.5194/acp-14-447-2014, 2014.

Sihto, S.-L., Kulmala, M., Kerminen, V.-M., Dal Maso, M., Petäjä, T., Riipinen, I., Korhonen, H., Arnold, F., Janson, R., Boy, M., Laaksonen, A., and Lehtinen, K. E. J.: Atmospheric sulphuric acid and aerosol formation: implications from atmospheric measurements for nucleation and early growth mechanisms, Atmos. Chem. Phys., 6, 4079–4091, doi:10.5194/acp-6-4079-2006, 2006.

Spracklen, D. V., Carslaw, K. S., Kulmala, M., Kerminen, V.-M., Mann, G. W., and Sihto, S.-L.: The contribution of boundary layer nucleation events to total particle concentrations on regional and global scales, Atmos. Chem. Phys., 6, 5631–5648, doi:10.5194/acp-6-5631-2006, 2006.

Spracklen, D. V., Carslaw, K. S., Kulmala, M., Kerminen, V.-M., Sihto, S.-L., Riipinen, I., Merikanto, J., Mann, G. W., Chipperfield, M. P., Wiedensohler, A., Birmili, W., and Li-

Title Page

Abstract | Introduction

Conclusions | References

Tables | Figures

|◀ | ▶|

◀ | ▶

Back | Close

Full Screen / Esc

Printer-friendly Version

Interactive Discussion

havainen, H.: Contribution of particle formation to global cloud condensation nuclei concentrations, Geophys. Res. Lett., 35, L06808, doi:10.1029/2007gl033038, 2008.

Spracklen, D. V., Carslaw, K. S., Merikanto, J., Mann, G. W., Reddington, C. L., Pickering, S., Ogren, J. A., Andrews, E., Baltensperger, U., Weingartner, E., Boy, M., Kulmala, M., Laakso, L., Lihavainen, H., Kivekäs, N., Komppula, M., Mihalopoulos, N., Kouvarakis, G., Jennings, S. G., O'Dowd, C., Birmili, W., Wiedensohler, A., Weller, R., Gras, J., Laj, P., Sellegri, K., Bonn, B., Krejci, R., Laaksonen, A., Hamed, A., Minikin, A., Harrison, R. M., Talbot, R., and Sun, J.: Explaining global surface aerosol number concentrations in terms of primary emissions and particle formation, Atmos. Chem. Phys., 10, 4775–4793, doi:10.5194/acp-10-4775-2010, 2010.

Unger, N.: On the role of plant volatiles in anthropogenic global climate change, Geophys. Res. Lett., 41, 8563–8569, doi:10.1002/2014GL061616, 2014.

Yli-Juuti, T., Nieminen, T., Hirsikko, A., Aalto, P. P., Asmi, E., Hõrrak, U., Manninen, H. E., Patokoski, J., Dal Maso, M., Petäjä, T., Rinne, J., Kulmala, M., and Riipinen, I.: Growth rates of nucleation mode particles in Hyytiälä during 2003–2009: variation with particle size, season, data analysis method and ambient conditions, Atmos. Chem. Phys., 11, 12865–12886, doi:10.5194/acp-11-12865-2011, 2011.

Yu, F.: A secondary organic aerosol formation model considering successive oxidation aging and kinetic condensation of organic compounds: global scale implications, Atmos. Chem. Phys., 11, 1083–1099, doi:10.5194/acp-11-1083-2011, 2011.

Zhang, Q., Jimenez, J. L., Canagaratna, M. R., Allan, J. D., Coe, H., Ulbrich, I., Alfarra, M. R., Takami, A., Middlebrook, A. M., Sun, Y. L., Dzepina, K., Dunlea, E., Docherty, K., DeCarlo, P. F., Salcedo, D., Onasch, T., Jayne, J. T., Miyoshi, T., Shimono, A., Hatakeyama, S., Takegawa, N., Kondo, Y., Schneider, J., Drewnick, F., Borrmann, S., Weimer, S., Demerjian, K., Williams, P., Bower, K., Bahreini, R., Cottrell, L., Griffin, R. J., Rautiainen, J., Sun, J. Y., Zhang, Y. M., and Worsnop, D. R.: Ubiquity and dominance of oxygenated species in organic aerosols in anthropogenically-influenced Northern Hemisphere midlatitudes, Geophys. Res. Lett., 34, L13801, doi:10.1029/2007GL029979, 2007.

Zhang, X., Pandis, S. N., and Seinfeld, J. H.: Diffusion-limited versus quasi-equilibrium aerosol growth, Aerosol Sci. Technol., 46, 874–885, doi:10.1080/02786826.2012.679344, 2012.

Table 1. Global annual mean fluxes of secondary organic material, in the model surface layer, to the aerosol size distribution in GLOMAP. D_g is the geometric mean diameter for each mode.

New particle formation	Distribution of secondary organic material		Smaller than 100 nm		Larger than 100 nm	
			Nucleation ($D_g < 10$ nm)	Aitken ($10 < D_g < 100$ nm)	Accumulation (100 nm $< D_g < 1$ µm)	Coarse ($D_g > 1$ µm)
ACT	Kinetic (KinSOA)	Percentage of total flux	0.26 %	20.94 %	78.26 %	0.55 %
		Annual total flux	4.28 Tg (SOA) a^{-1} 6.77×10^{-12} ng (SOA) particle^{-1} s^{-1}		15.92 Tg (SOA) a^{-1} 1.50×10^{-11} ng (SOA) particle^{-1} s^{-1}	
	Thermodynamic (ThermSOA)	Percentage of total flux	0.00 %	18.71 %	81.24 %	0.04 %
		Annual total flux	3.77 Tg (SOA) a^{-1} 4.06×10^{-12} ng (SOA) particle^{-1} s^{-1}		16.38 Tg (SOA) a^{-1} 1.81×10^{-11} ng (SOA) particle^{-1} s^{-1}	
	50 % kinetic 50 % thermodynamic	Percentage of total flux	0.19 %	20.92 %	78.49 %	0.40 %
	(SplitSOA)	Annual total flux	4.27 Tg (SOA) a^{-1} 6.10×10^{-12} ng (SOA) particle^{-1} s^{-1}		15.94 Tg (SOA) a^{-1} 1.53×10^{-11} ng (SOA) particle^{-1} s^{-1}	
ORG	Kinetic (KinSOA)	Percentage of total flux	0.87 %	24.32 %	74.35 %	0.45 %
		Annual total flux	5.11 Tg (SOA) a^{-1} 3.78×10^{-12} ng (SOA) particle^{-1} s^{-1}		15.17 Tg (SOA) a^{-1} 1.04×10^{-11} ng (SOA) particle^{-1} s^{-1}	
	Thermodynamic (ThermSOA)	Percentage of total flux	0.00 %	18.80 %	81.12 %	0.08 %
		Annual total flux	3.80 Tg (SOA) a^{-1} 1.63×10^{-12} ng (SOA) particle^{-1} s^{-1}		16.40 Tg (SOA) a^{-1} 1.69×10^{-11} ng (SOA) particle^{-1} s^{-1}	
	50 % kinetic 50 % thermodynamic	Percentage of total flux	0.67 %	23.55 %	75.44 %	0.34 %
	(SplitSOA)	Annual total flux	4.91 Tg (SOA) a^{-1} 3.21×10^{-12} ng (SOA) particle^{-1} s^{-1}		15.37 Tg (SOA) a^{-1} 1.10×10^{-11} ng (SOA) particle^{-1} s^{-1}	

Table 2. Global annual mean change to CDNC, calculated using a globally uniform updraught velocity of $0.2\,\mathrm{m\,s^{-1}}$, in the model level corresponding to low-level cloud base (mean pressure of approx. 900 hPa), and first AIE, due to biogenic SOA in GLOMAP and TOMAS using the kinetic and thermodynamic approaches.

Nucleation mechanism	Background (without biogenic SOA) global annual mean CDNC $(\mathrm{cm^{-3}})$	Distribution of secondary organic material	ΔCDNC	AIE $(\mathrm{W\,m^{-2}})$	DRE $(\mathrm{W\,m^{-2}})$
ACT	185.2	Kinetic	+6.3 (+3.4 %)	−0.07	−0.10
		Thermodynamic	+2.6 (+1.4 %)	+0.01	−0.11
		50 % kinetic 50 % thermodynamic	+5.9 (+3.2 %)	−0.05	−0.11
ORG	165.2	Kinetic	+41.5 (+25.1 %)	−0.78	−0.08
		Thermodynamic	+33.0 (+20.0 %)	−0.59	−0.08
		50 % kinetic 50 % thermodynamic	+40.3 (+24.4 %)	−0.75	−0.09

Table 3. Global annual mean change to cloud droplet number concentration (CDNC), calculated using five globally uniform updraught velocities, in the model level which corresponds to low-level cloud base (mean pressure of approximately 900 hPa), and first aerosol indirect effect (AIE), reported to 2 decimal places, resulting from the inclusion of biogenic SOA in GLOMAP using the kinetic and thermodynamic approaches. The mean values are calculated assuming that all updraught velocities are equally likely.

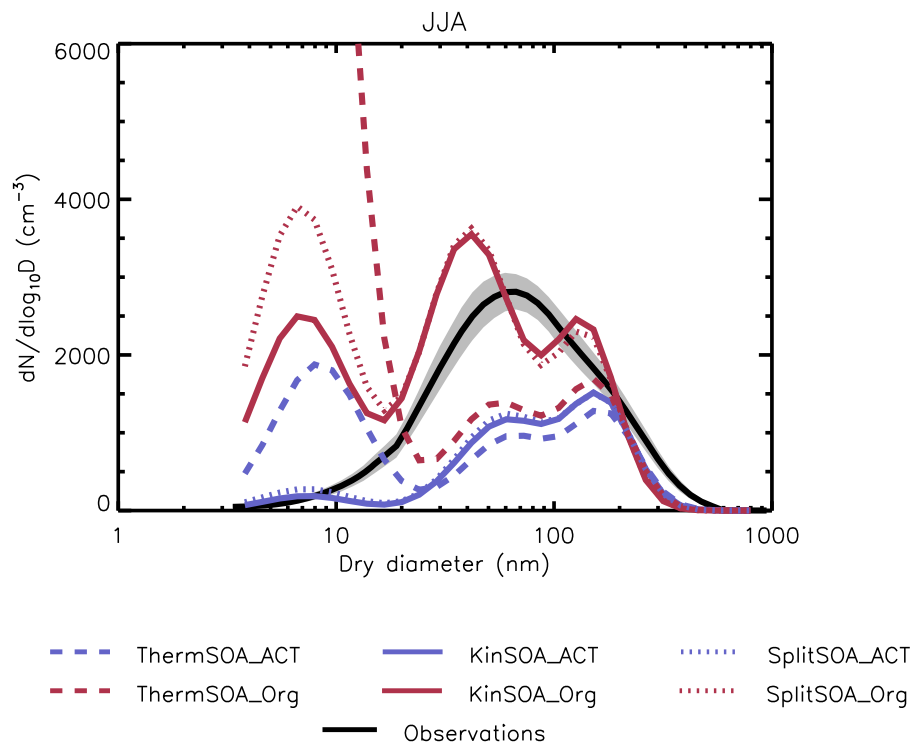| Nucleation mechanism	Updraught velocity ($m\,s^{-1}$)	Distribution of secondary organic material			
		Kinetic		Thermodynamic	
		ΔCDNC (cm^{-3})	AIE ($W\,m^{-2}$)	ΔCDNC (cm^{-3})	AIE ($W\,m^{-2}$)
ACT	0.1	+2.7 (+2.0 %)	−0.04	+0.6 (+0.5 %)	+0.02
	0.2	+6.3 (+3.4 %)	−0.07	+2.6 (+1.4 %)	+0.01
	0.3	+9.1 (+4.3 %)	−0.08	+4.4 (+2.1 %)	0.00
	0.4	+11.3 (+4.9 %)	−0.08	+6.0 (+2.6 %)	−0.01
	0.5	+12.9 (+5.3 %)	−0.08	+7.2 (+3.0 %)	−0.01
	Mean	**+8.4 (+4.0 %)**	**−0.07**	**+4.2 (+1.9 %)**	**+0.004**

Figure 1. Simulated and measured (multi-annual; 1996–2006) mean aerosol number size distribution at a boreal forest site (Hyytiälä, Finland) during June-July-August. The grey shaded region indicates ±1 SD from the JJA mean size distribution over the years 1996–2006. Simulations show the sensitivity to nucleation mechanism: activation (blue), organic (red) and condensation assumptions: kinetic (solid), thermodynamic (dashed), 50 % split kinetic-thermodynamic (dotted).

Figure 2. Annual mean percentage change to CDNC (using a uniform updraught velocity of $0.2\,\mathrm{m\,s^{-1}}$) from biogenic SOA in GLOMAP, in the model level which corresponds to low-level cloud base (mean pressure of approximately 900 hPa); SOA is distributed kinetically (**a** and **c**), thermodynamically (**b** and **d**). Simulations use either an activation (**a** and **b**) or organically mediated (**c** and **d**) new particle formation mechanism.
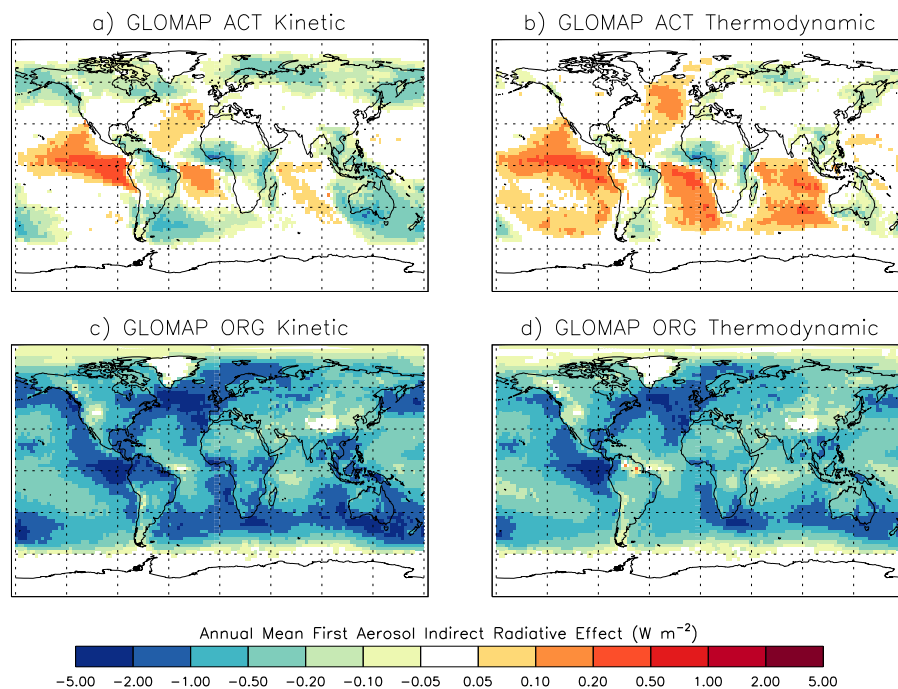
Figure 3. Annual mean first AIE ($\mathrm{W\,m^{-2}}$) from biogenic SOA in GLOMAP when SOA is distributed kinetically (**a** and **c**), thermodynamically (**b** and **d**). Simulations use either an activation (**a** and **b**) or organically mediated (**c** and **d**) new particle formation mechanism.